Unveiling the Pharmacological Mechanism of Cosmos caudatus Compounds as Lung Cancer Drug Candidates: Pharmacology Networking, Molecular Docking, and Experimental Validation

Abdul Halim Umar

ahuhalim76@yahoo.com

Almarisah Madani University

Citra Surya Ningsi Biringallo

Almarisah Madani University

Pratiwi Intan Tuyuwale

Almarisah Madani University

Anita Kila

Almarisah Madani University

Karin Dian Febyola

Almarisah Madani University

Reny Syahruni

Almarisah Madani University

Wahyu Hendrarti

Almarisah Madani University

Mohamad Rafi

IPB University

Diah Ratnadewi

IPB University

Research Article

Keywords: AKT1, bioinformatics, drug discovery, lung neoplasms, PIP3 activates AKT signaling

Posted Date: April 3rd, 2025

DOI: https://doi.org/10.21203/rs.3.rs-5961891/v1

Additional Declarations: No competing interests reported.

Version of Record: A version of this preprint was published at Journal of Pharmaceutical Innovation on April 21st, 2025. See the published version at https://doi.org/10.1007/s12247-025-09989-0.

Abstract

Cosmos caudatus is a traditional Indonesian medicinal plant commonly used in the treatment of cancer, hypertension, diabetes, osteoporosis, and other potential health conditions. However, the mechanisms behind its compounds, targets, diseases, disease pathways, and their molecular profiles in treating lung cancer remain unclear. Therefore, a comprehensive approach is required to study these mechanisms by integrating metabolomics, bioinformatics, and in vitro experimental validation to explore the active compounds, targets, diseases, disease pathways, and molecular mechanisms involved in the treatment of lung cancer. The metabolomic approach identified 66 compounds in the leaves, of which 13 met the criteria for gastrointestinal drugs. The compounds 3',4',5,7-tetrahydroxyflavone, AKT1 target, lung neoplasms diseases, and PIP3 activating AKT signalling pathway, each became the core target with the highest degree value in the pharmacological network formed. In the protein-protein interaction (PPI) network, AKT1 again became the core target with the highest degree value. Gene Ontology (GO) functional enrichment analysis revealed that the biological processes, molecular functions, cellular components, and KEGG pathways in lung cancer were phosphorylation, cytoplasm, protein binding, and cancer pathways, respectively. The three compounds with the best binding energy and hydrogen bonding were 3',4',5,7-tetrahydroxyflavone-AKT1 (9C1W), gamma-mangostin-EGFR (3P0V), and cratoxyarborenone E-TNF (1XU1), with binding energies of -10.8, -8.9, and − 9.6 kcal/mol, respectively. The methanol extracts inhibited A549 cells at a concentration of 156.12 µg/mL. The combination of these methods provides insights into the pharmacological mechanisms of *C. caudatus* compounds in the treatment of lung cancer.

Introduction

According to data from the Global Burden of Cancer Study, lung cancer is the leading cause of cancer-related deaths, accounting for 1.8 million deaths worldwide in 2020, with a 5-year survival rate of only 10–20% [1]. In Indonesia, there were 34,783 lung cancer cases and 30,843 deaths in 2020 [2]. It is projected that by 2040, the number of new lung cancer cases will rise to approximately 28 million, with 16 million people expected to die from the disease. Lung cancer management typically involves a combination of therapy, surgery, radiation, and chemotherapy. Among these, chemotherapy plays an important role in reducing cancer-related symptoms and extending patients' life expectancy. However, chemotherapy drugs are expensive and come with significant side effects, including hepatobiliary disorders, gastrointestinal issues, cardiotoxicity, and a weakened immune system. Additionally, chemotherapeutic drugs often have poor systemic distribution and low bioavailability, which can lead to drug resistance (MDR) and therapeutic failure [3, 4]. Given the severe side effects, there is a need to develop more effective and cost-efficient therapies for lung cancer with fewer side effects.

One potential approach is the use of medicinal plants, such as *Cosmos caudatus* Kunth (Asteraceae) [5]. In Indonesia, this plant is known as Kenikir. Its leaves are commonly used as fresh vegetables and in herbal tea drinks [6–8]. The plant is known to contain various bioactive compounds, including chlorogenic acid, neochlorogenic acid, cryptochlorogenic acid, arabinofuranosides, glucosides,

rhamnosides, rutinosides, quercetin, caffeic acid, ferulic acid, and essential oils such as γ-cadine and caryophyllene, all of which show potential for treating cancer, hypertension, diabetes, osteoporosis, and for their antioxidant, antifungal, antibacterial, and other beneficial functions [6–11]. In addition to its pharmacological properties, this plant is reported to have very low toxicity, making it safe for consumption [12]. *Cosmos caudatus* has also been shown to exhibit cytotoxic effects in vitro against cervical cancer [13], human colorectal carcinoma cells [14], and human oral squamous carcinoma (HSC)-3 cells [15], In silico studies have revealed its potential anti-breast cancer effects through the interaction of the compound 5-O-methylvisammioside with the SLC2A1 ligand [16]. However, the mechanisms of its compounds, targets, diseases, and disease pathways, as well as their molecular profiles in the treatment of lung cancer, remain unclear.

The metabolomics and bioinformatics approach is a method that provides scientific support and innovative technologies for rational clinical drug development by combining metabolite profiling, pharmacological networks, and molecular docking [16–18]. Metabolite profiling using LC-HRMS is an efficient technique for compound identification that requires minimal sample quantities and provides rapid results [8, 19, 20]. Pharmacological networks predict interactions between compounds, target genes, diseases, and disease pathways, offering insights into the mechanisms involved in treating specific diseases [21–23]. Additionally, molecular docking can predict the optimal interaction and binding affinity between ligands and receptors [16]. In this study, we explored the active compounds, targets, diseases, disease pathways, and molecular mechanisms of the active compounds in *C. caudatus* for treating lung cancer through pharmacological networks, molecular docking, and in vitro experimental validation.

Materials and methods

Samples collection

Samples of *Cosmos caudatus* were collected from Leang-Leang Village, Bantimurung District, Maros Regency, South Sulawesi Province. A total of 2 kg of plant material was gathered and processed into simplicia powder. The samples were then extracted with methanol using the maceration method for 5 days. The resulting extract was filtered and concentrated using a rotary evaporator. Subsequently, partitioning of the extract was performed with n-hexane and chloroform solvents. Further, the compounds in each extract were identified using liquid chromatography-mass spectrometry (LC-MS/MS).

Metabolite analysis with LC-HRMS

Metabolite analysis was performed using QTOF LC-MS/MS with ultra-performance liquid chromatography (UPLC) (Acquity UPLC H-class system, Waters, USA) and a mass spectrometer (Xevo G2-S QTOF, Waters, USA), following the method described by Rafi et al. [8] with slight modifications. The mass spectrometer was operated in mass spectrometer mode and in both positive and negative electrospray ionization modes.

LC-MS/MS data in *.raw file format were imported into Abf Converter 4.0.0. (format *.abf) and MS FileReader 2.2.62, MS-DIAL ver. 3.82 (for peak detection, filtering, and alignment), and MSFinder. Additionally, online tools such as CFM-ID (https://cfmid.wishartlab.com/), MetFrag, and CSI: FingerID (https://www.csi-fingerid.uni-jena.de/) were used for compound fragmentation pattern analysis. The peak detection parameters were set with a minimum peak height of 10,000 (Orbitrap), a linear weighted moving average smoothing method, and a minimum peak width. Identification was performed using an in-house database with a 75% cut-off score, considering adduct types [M + H]+ and [M – H]–, and alignment was based on a reference blank [19].

Prediction of compound absorption

The compound absorption parameters (physicochemical properties, lipophilicity) following the Lipinski Rule of Five were predicted using Molinspiration software, the Lipinski Rule of Five (Ro5) (http://www.scfbio-iitd.res.in/), admetSAR 2.0 (http://lmmd.ecust.edu.cn/admetsar2/), and SwissADME (http://www.swissadme.ch/index.php) [17]. To ensure consistent screening criteria, all obtained compounds were filtered based on oral bioavailability (OB) ≥ 30% and drug-likeness (DL) ≥ 0.18 [24].

Exploration of *Cosmos caudatus'* bioactive compounds

Bioactive compounds of *C. caudatus* were identified through LC-HRMS analysis and a review of previous research literature. The chemical structures and compound IDs were analyzed using online platforms such as PubChem (https://pubchem.ncbi.nlm.nih.gov/), KNApSAcK Family (http://www.knapsackfamily.com/KNApSAcK_Family/), ChemSpider (https://www.chemspider.com/), SpectraBase (https://spectrabase.com/), and MOLBASE (https://key.molbase.cn/). These databases provided data on compounds, isomeric/canonical SMILES, and compound IDs [17].

Screening and target prediction of *Cosmos caudatus* compounds

Target determination of *C. caudatus* compounds was conducted using the SwissTargetPrediction database platform (http://swisstargetprediction.ch/). Additionally, lung cancer marker targets were screened using the OMIM database, GeneCards, DrugBank, PharmGKB, DisGeNet, and the Therapeutic Target Database (TTD) platforms with the keyword “Lung cancer.”

Screening lung cancer targets

Lung cancer targets obtained from the OMIM database, GeneCards, DrugBank, PharmGKB, DisGeNet, and TTD were then analyzed using the Draw Venn Diagram platform (https://bioinformatics.psb.ugent.be/webtools/Venn/) [25]. The identified targets were further used to screen *C. caudatus* compounds that could potentially serve as lung cancer markers.

Disease screening and prediction of disease pathways

The selected targets were further analyzed using the Therapeutic Target Database (TTD) (https://db.idrblab.org/ttd/) [26] and the Comparative Toxicogenomics Database (CTD) (http://ctdbase.org/) [27] to predict disease outcomes and pathways related to lung cancer. The keyword “cancer” was used to facilitate the analysis.

Construction of Plant-compound-target-disease-pathway networks

The previously identified compounds, targets, diseases, and disease pathways were imported into Cytoscape 3.10.1 software (https://cytoscape.org/) to create multi-compound–multi-target, multi-target–multi-disease, and multi-disease–multi-disease pathway networks for visualization. These networks were then analyzed using the Network Analyzer tool [18]. Degree, betweenness centrality, and closeness centrality values were used as topological features to evaluate the network interactions.

Construction of protein-protein interaction (PPI) networks

Gene/protein interactions for the core targets derived from *C. caudatus* were identified using STRING version 11.0 (https://string-db.org). Overlaps were predicted with a minimum required interaction score of 0.900 (for *Homo sapiens*). PPI (protein-protein interaction) results with a threshold score of >0.4 were then exported to Cytoscape 3.10.1 via the “send network to Cytoscape” feature for further visualization of the PPI networks. Degree values were used to highlight the importance of core targets in the PPI network analysis. In the PPI networks, edges represent protein-protein associations, with the number of edges indicating the strength of the correlation [16].

Gene ontology (GO) and pathway (KEGG) analysis

Data obtained from target screening were entered into the DAVID Bioinformatics Resources 6.8 server (https://david.ncifcrf.gov/home.jsp) and STRING version 11.0 (https://string-db.org) to determine the biological processes (BP), cellular components (CC), and molecular functions (MF) of the identified targets. The data were then processed and visualized using the SRplot platform (http://www.bioinformatics.com.cn/en), presenting Gene Ontology (GO) results. Important biological pathways were analyzed using the Kyoto Encyclopedia of Genes and Genomes (KEGG). Items with p-values and false discovery rates (FDR) < 0.01 were considered significant. The top 15 GO or KEGG terms were selected for further analysis [16].

Molecular docking analysis

Three-dimensional (3-D) structures and compound CIDs of ligands were obtained from the PubChem database, while proteins (receptors) corresponding to the target (specific to *Homo sapiens*) were retrieved from the RCSB Protein Data Bank (http://www.rcsb.org/). Ligand and protein optimization was performed using Chimera 1.17.3 (UCSF) with the MMFF94 force field and PyMOL version 2.5 (https://pymol.org/2/). The optimization results for both ligands and receptors were analyzed for binding energy, RMSD, amino acid residues, and bond types using PyRx AutoDock Vina (https://pyrx.sourceforge.io/) version 0.9.x. Furthermore, PyMOL and BIOVIA Discovery Studio Visualizer

(https://www.3dsbiovia.com) were used to visualize the ligand-receptor docking results [18]. The best candidates were selected based on the lowest binding energy (high docking value) and hydrogen bond interactions. Additionally, the RMSD value (≤2 Å) was used as a docking validation parameter [28].

Cell culture

The A549 cell line (American Type Culture Collection (ATCC, USA) was cultured in Dulbecco's Modified Eagle Medium (DMEM) supplemented with 10% fetal bovine serum and 5 mM glutamine. The cells were maintained in tissue culture flasks in a 5% CO2 incubator with 95% humidity at 37°C. For further analysis, A549 cells were seeded in 96-well tissue culture plates at a density of 25,000 cells per well [29].

Resazurin chemo-sensitivity assay

The Resazurin assay, also known as Alamar Blue dye, assesses the reduced oxidative environment of cells using fluorometric analysis to precisely quantify metabolic activity. Resazurin is a fluorescent redox dye that transitions from blue to pink when metabolically active cells reduce it to resorufin. This assay was used to evaluate the anticancer activity of methanol, n-hexane, and chloroform extracts on A549 lung cancer cells, following the method of Gurning et al. [30] and Gao et al. [29], with some modifications. For the assay, a stock solution of 200,000 µg/mL was prepared using 2% ethanol solvent. Eight 1.5 mL microtubes were used to create eight different concentrations ranging from 1000 µg/mL to 7.81 µg/mL. The A549 cell cultures were removed from the incubator, and the media was discarded from the wells. The plate was then labeled, and 100 µL of each sample was added to the respective wells, followed by incubation for 48 hours. Afterward, the percentage of inhibition for each concentration was determined, and the IC_{50} value was calculated to assess the anticancer activity of the test extracts. Doxorubicin was used as a positive control.

Results

Identification, prediction of bioavailability, and druglikeness of compounds

A total of 66 active compounds were identified from the LC-MS/MS analysis of methanol, chloroform, and n-hexane extracts (Table 1). Of these, 13 compounds met the bioavailability and drug-likeness criteria. The parameters related to the five Lipinski rules (MW, nON, nOHNH, MR, and LogP) for these compounds are summarized in Table S1. The 13 compounds were primarily composed of polyphenol groups, along with other groups such as terpenes and polyketides (Table S2).

Screening and target prediction of *Cosmos caudatus* compounds against lung cancer

Using the online platforms DisGeNet, DrugBank, GeneCards, PharmGKB, and the Therapeutic Target Database (TTD), a total of 1224, 29, 532, 29, and 30 targets were identified, respectively, resulting in 1844 unique targets (Fig. 1). Duplicate targets across the five databases were removed. The lung cancer targets and compound targets were then intersected, yielding 48 common targets.

Disease screening and prediction of disease pathways

Disease screening using the Therapeutic Target Database (TTD) and the Comparative Toxicogenomics Database identified 58 diseases and 288 pathways after searching and screening disease and pathway data.

Plant–compound–target–disease–pathway networks

At the pharmacological network stage, 255 nodes and 1318 edges were obtained (Fig. 2). This result represents the integration of the Plant–Compound, Compound–Target, Target–Disease, and Disease–Pathway networks. Based on the analysis of three compounds, the targets, diseases, and pathways with the highest degree in the lung cancer network were identified as follows: compounds 3',4',5,7-tetrahydroxyflavone (18), cratoxyarborenone E (16), and gamma-mangostin (13); targets AKT1 (40), EGFR (33), and ABCG2 (32); diseases lung neoplasms (79), neoplasm metastasis (74), and lung injury (66); and pathways such as PIP3 activates AKT signaling (54), NCAM signaling for neurite outgrowth (54), and B cell receptor signaling pathway (49) (Tables S3–S6).

Protein-protein interaction (PPI) networks

The intersection data of lung cancer targets and compounds were analyzed for PPI. In the PPI network (Fig. 3), 29 nodes and 145 edges were formed, with an average node degree of 10.0 and a local clustering coefficient of 0.653. The topological features of betweenness centrality, closeness centrality, and degree are provided in Table S7. The ten proteins with the highest degree values are EGFR (33), AKT1 (32), STAT3 (29), TNF (28), GSK3B (23), MDM2 (23), RELA (23), PIK3CA (20), IL1B (19), and HDAC1 (19). These nodes in the PPI network represent key linkages involved in lung cancer progression.

Gene ontology (GO) and pathway (KEGG) of lung cancer

GO analysis of target genes, using the BP, MF, and CC parameters, identified positive regulation of phosphorylation, cytoplasm, and protein binding as the top terms (top 10), respectively. The KEGG pathway analysis revealed pathways in cancer as the most significant pathway. This analysis was conducted with a p-value threshold of <0.01 (top 20). The results of the GO and KEGG analyses are presented in Fig. 4.

Molecular docking

A total of three compounds (3‘,4’,5,7-tetrahydroxyflavone, gamma-mangostin, and cratoxyarborenone E) with the highest degree in the pharmacological network, and three core targets (AKT1, EGFR, and TNF) identified from protein-protein interaction analysis, were selected for the molecular docking stage to assess the interactions, binding energy, and amino acid residues involved between the targets and compounds (Table 2).

Based on the visualization results, the three compounds interact with each of the three targets through various types of bonds, including van der Waals, conventional hydrogen bonds, unfavorable donor-donor interactions, Pi-sigma, Pi-pi stacked, amide Pi-stacked, alkyl, and Pi-alkyl interactions (Fig. 5). The lower the binding energy between the compound and the receptor, the more stable the docking result. The three compounds with the best binding energies were 3‘,4’,5,7-tetrahydroxyflavone-AKT1 (9C1W) at –10.8 kcal/mol, gamma-mangostin-AKT1 (9C1W) at –10.0 kcal/mol, and cratoxyarborenone E-TNF (1XU1) at –9.6 kcal/mol. However, the gamma-mangostin-EGFR (3P0V) interaction did not involve hydrogen bonds, so it was considered an alternative with a binding energy of –8.9 kcal/mol. All three compounds had RMSD values below 2 Å, with values of 0.82 Å, 1.25 Å, and 0.98 Å, respectively.

In vitro cytotoxicity

The *in vitro* cytotoxicity test was conducted using three extract samples (methanol, chloroform, and n-hexane solvents), each tested across an 8-concentration series to determine the IC_{50} value of each sample. Fig. 6 presents the IC_{50} values of the extracts against A549 cells *in vitro*. The methanol extract demonstrated the highest inhibition (lowest IC_{50}) against the test cells, with an IC_{50} value of 156.12 µg/mL, compared to the chloroform and n-hexane extracts, which showed moderate cytotoxic effects after 48 hours.

Discussion

Based on the results from LC-HRMS analysis and a literature review, 66 active compounds were identified in *C. caudatus* leaves. After screening, 13 active compounds were selected for having favorable ADME and drug-likeness parameters. This initial evaluation of the drug properties of natural materials can enhance the success rate of drug development, reduce associated costs, minimize side effects and toxicity, and guide the rational clinical use of these drugs [16, 17]. Additionally, this evaluation helps confirm the potential of these compounds as drug candidates for treating lung cancer.

In the pharmacological network stage, the compounds, targets, diseases, and pathways with the highest degree were identified as follows: 3',4',5,7-tetrahydroxyflavone (compound); AKT1 (target); lung neoplasms (disease); and PIP3 activating AKT signaling (pathway). The degree in the network reflects the number of targets associated with each node based on topological analysis; a higher degree indicates a more significant role for the component or target [31, 32]. The compound 3',4',5,7-tetrahydroxyflavone, a flavonoid, has been extensively reported for its anticancer properties, particularly in the treatment of lung cancer [33–38]. AKT1 plays a critical role in the pathogenesis of lung neoplasms. Inhibition of AKT1 regulates cell proliferation, especially in lung cancer [39, 40]. AKT1 expression is significantly elevated in lung cancer patients [40]. The PI3K/AKT/mTOR signaling pathway is one of the most crucial intracellular signaling pathways. Specifically, phosphatidylinositol-3,4,5-triphosphate (PIP3), a second messenger generated by PI3K activity, activates the serine-threonine kinase AKT. This, in turn, regulates essential cellular functions such as quiescence, survival, cell cycle

progression, and apoptosis under both healthy and pathological conditions, including lung cancer [39, 41, 42].

Protein-protein interactions revealed that AKT1 and EGFR had the highest degree of interaction. The AKT pathway regulates cell growth, adhesion, migration, survival, and other cellular processes. Overactivation of AKT1 signaling can promote cell proliferation and the tumorigenesis of lung cancer [35, 43, 44]. EGFR is a transmembrane receptor tyrosine kinase. Increased EGFR kinase activity leads to the hyperactivation of several signaling pathways, including MAPK/ERK, PI3K/Akt/mTOR, and IL-6/JAK/STAT3, all of which contribute to lung cancer cell tumorigenesis [45].

In this study, gene ontology analysis in the biological process (BP) category revealed that phosphorylation had the highest enrichment score. Phosphorylation is one of the most common post-translational modifications involved in regulating various biological processes such as cell division, protein degradation, signal transduction, gene expression regulation, and protein interactions [46, 47]. Additionally, phosphorylation is involved in the overexpression of kinases, which plays a key role in the oncogenesis of various tumors. Phosphorylation pathways critical to cancer development include MAPK, PI3K/AKT, tyrosine kinase, cadherin-catenin complex, cyclin-dependent kinase, NF-kappaB and IkappaB proteins, and TGF-β signaling [46–48]. The cellular component (CC) analysis pointed to the plasma membrane. Cytoplasmic vacuolation is induced during cell proliferation, particularly in cancer cells [49]. Eosinophilic cytoplasm also increases with tumor cell proliferation [50–52]. In the molecular function (MF) category, protein binding was shown to promote the expression of genes related to tumor proliferation, metastasis, and apoptosis suppression [53, 54]. Binding proteins are potential targets for lung cancer therapy [54, 55]. KEGG pathway analysis identified human cancer pathways, with the PIP3-activated AKT signaling pathway as a core target, where activation of this pathway facilitates cancer cell proliferation and metastasis [41].

Molecular docking is a computational technique used to identify interactions between components (ligands) and targets (receptors) in tissue, improving the accuracy of tissue-level predictions. At the cellular and animal levels (using a mouse xenograft model), the compound 3',4',5,7-tetrahydroxyflavone has shown potential as a lung anticancer drug. It inhibits the association of Hsp90 with the EGF receptor, thereby preventing PI3K/Akt/mTOR signaling, which leads to apoptosis of lung cancer cells [34, 56]. This compound also reduces A549 cell migration and overexpresses miR-106a-5p [37, 38]. Gamma-mangostin, found in *Garcinia mangostana*, along with its alpha and beta mangostin derivatives, has been reported to have anti-metastatic effects on cancer cells, especially A549 lung cancer cells [57], as well as anti-melanoma effects on the SK-MEL-28 cell line [58], and the ability to reduce liver fibrosis via Sirtuin 3-superoxide-high mobility group box 1 [59]. The compound cratoxyarborenone E, a class of xanthones, was also identified in this plant. It has been isolated from *Cratoxylum glaucum* and has shown antimalarial [60, 61] and anti-amoebic activities [62].

The ligands 3‘,4’,5,7-tetrahydroxyflavone, gamma-mangostin, and cratoxyarborenone E interact with AKT1 (AKT serine/threonine kinase 1), EGFR (epidermal growth factor receptor), and TNF (tumor

necrosis factor) receptors through several types of bonds, one of which is hydrogen bonding. The strength and weakness of ligand binding affinity to the receptor are strongly influenced by hydrogen bonds [63, 64]. AKT1 is a protein kinase B that plays a crucial role in tumorigenesis and its progression [65]. This protein has been identified in breast cancer, ovarian cancer, colorectal cancer, and lung cancer [66]. Inhibiting AKT1 activity can promote cancer cell apoptosis and inhibit tumor growth [39, 67, 68]. EGFR, a transmembrane glycoprotein, is a member of the ERBB receptor tyrosine kinase superfamily. It binds to its cognate ligands, leading to tyrosine phosphorylation and receptor dimerization, which in turn induces uncontrolled cell proliferation [69, 70]. EGFR is involved in cell signaling pathways that control cell division and survival [71]. Inhibiting EGFR expression can prevent uncontrolled tumor proliferation and growth [72–74]. TNF promotes tumor progression and disables the antitumor immune response. Most cancers adapt to the TNF response, creating an imbalance between cell death and survival, which leads to uncontrolled cell proliferation [75], This includes activation of nuclear factor kappa-light-chain-enhancer of activated B cells (NF-κB), which increases the expression of several anti-apoptotic proteins [75, 76].

The IC_{50} value is commonly used as a cell cytotoxic parameter in natural material testing. The cytotoxic effects are classified as follows: strong cytotoxic (IC_{50} < 21 µg/mL), moderate (IC_{50} 21–200 µg/mL), weak (IC_{50} 201–500 µg/mL), and non-cytotoxic (IC_{50} > 501 µg/mL) [77, 78]. Despite its moderate anticancer activity (IC_{50} = 156.12 µg/mL), this natural product can be used as a cancer prevention agent, particularly for lung cancer. As the material is still in the form of crude extracts, further refinement is needed to obtain specific compounds with higher cytotoxic activity against A549 lung cancer cells, particularly methanol extracts, which are rich in polyphenolic compounds.

Conclusions

Combination studies involving metabolomics, bioinformatics, and *in vitro* biological evaluations can provide a comprehensive and holistic perspective on the mechanism of *C. caudatus* compounds as an alternative treatment for lung cancer. Active components such as 3’,4’,5,7-tetrahydroxyflavone, gamma-mangostin, and cratoxyarborenone E can bind to AKT1 (9C1W), EGFR (3P0V), and TNF (1XU1), playing a role in the biological process of phosphorylation within the cytoplasm, and contributing to molecular functions through protein binding, as well as impacting cancer-related pathways in KEGG. Although this study presents promising results, its limitations should be acknowledged. Therefore, further investigations are needed to validate its clinical applicability.

Declarations

Conflict of interest

The authors declare no competing interests

Author Contribution

A.H.U Conceptualization, Formal analysis, Investigation, Methodology, Software, Validation, Roles/Writing - original draft, Writing - review & editing. C.S.N.B., P.I.T., A.K., and K.D.F Data curation, Formal analysis. R.S. and D.R. Conceptualization, Investigation, Validation, Writing - review & editing. W.H. and M.R. Validation, Writing - review & editing.

Acknowledgement

The authors would like to thank the Directorate General of Higher Education, Research and Technology through the Student Creativity Programme-Exact Research (PKM-RE) funding scheme.

Data availability

Data underlying this manuscript are provided in the supplementary material.

References

1. WHO. Lung cancer. 2023 [cited 2024 Sep 18]. Available from: https://www.who.int/news-room/fact-sheets/detail/lung-cancer
2. Asmara OD, Tenda ED, Singh G, Pitoyo CW, Rumende CM, Rajabto W, et al. Lung cancer in Indonesia. J Thorac Oncol. 2023;18:1134–45.
3. Anggraini CY, Kusumaningtyas TA, Junianandа M, Ningrum DWC, Febriansah R, Hermawansyah A. *In silico* and *in vitro* study *Selaginella doederleinii* herb extract as an antineoplastic on MCF-7 cells and formulation development of nano effervescent granule. Indones J Cancer Chemoprevention. 2023;14:128–38.
4. Khan A, Waheed Y, Kuttikrishnan S, Prabhu KS, El-Elimat T, Uddin S, et al. Network pharmacology, molecular simulation, and binding free energy calculation-based investigation of Neosetophomone B revealed key targets for the treatment of cancer. Front Pharmacol. 2024;15.
5. POWO. *Cosmos caudatus* Kunth | Plants of the World Online | Kew Science [Internet]. Plants of the World Online. 2024 [cited 2024 Nov 1]. Available from: http://powo.science.kew.org/taxon/urn:lsid:ipni.org:names:198324-1
6. Ahda M, Jaswir I, Khatib A, Ahmed QU, Syed Mohamad SNA. A review on *Cosmos caudatus* as A potential medicinal plant based on pharmacognosy, phytochemistry, and pharmacological activities. Int J Food Prop. 2023;26:344–58.
7. Afrianto WF, Tamnge F, Hidayatullah T, Hasanah LN. Local knowledge of plant-based nutrition sources from forgotten foods in Datengan Village, East Java, Indonesia. Asian J Ethnobiol. 2021;4.

8. Rafi M, Hayati F, Umar AH, Septaningsih DA, Rachmatiah T. LC-HRMS-based metabolomics to evaluate the phytochemical profile and antioxidant capacity of *Cosmos caudatus* with different extraction methods and solvents. Arab J Chem. 2023;16:105065.
9. Seyedreihani SF, Tan T-C, Alkarkhi AFM, Easa AM. Total phenolic content and antioxidant activity of Ulam raja (*Cosmos caudatus*) and quantification of its selected marker compounds: Effect of extraction. Int J Food Prop. 2017;20:260–70.
10. Firdaus M, Artanti N, Hanafi M, Hanafi M. Phytochemical constituents and *in vitro* antidiabetic and antioxidant properties of various extracts of kenikir (*Cosmos caudatus*) leaves. Pharmacogn J. 2021;13:890–5.
11. Yusoff NAH, Rukayadi Y, Abas F, Khatib A, Hassan M. Antimicrobial stability of *Cosmos caudatus* extract at varies pH and temperature, and compounds identification for application as food sanitiser. Food Res. 2021;5:83–91.
12. Herlina H, Amriani A, Sari IP, Apriani EF. Acute toxicity test of kenikir leaf (*Cosmos caudatus* H.B.K) ethanolic extract on Wistar white male rats with fixed dose procedure method and its effect on histopathology of pancreatic cells. J Advan Pharm Technol Res. 2021;12:157.
13. Dwira S, Fadhillah M, Azizah N, Putrianingsih R, Kusmardi K. Cytotoxic activity of ethanol and ethyl acetate extract of kenikir (*Cosmos caudatus*) against cervical cancer cell line (HELA). Res J Pharm Technol. 2019;12:1225–9.
14. Sia YS, Chern ZW, Hii SP, Tiu ZB, Arifin MA. Antimicrobial, antioxidant and cytotoxic activities of *Cosmos caudatus* extracts. Int J Eng Technol Sci. 2020;7:32–43.
15. Sandra F, Rizal MI, Dhaniar AY, Scania AE, Lee KH. *Cosmos caudatus* leaf extract triggers apoptosis of HSC-3 cancer cells by decreasing Bcl-2 and increasing Bax. Indones Biomed J. 2024;16:285–91.
16. Hendrarti W, Umar AH, Syahruni R, Rafi M, Kusuma WA. Deciphering the mechanism of action *Cosmos caudatus* compounds against breast neoplasm: A combination of pharmacological networking and molecular docking approach with bibliometric analysis. Indones J Sci Technol. 2024;9:527–56.
17. Syahruni R, Umar AH, Rahman HN, Kusuma WA. Exploration of *Annona muricata* (Annonaceae) in the treatment of hyperlipidemia through network pharmacology and molecular docking. Sains Malays. 2023;52:899–939.
18. Umar AH, Ratnadewi D, Rafi M, Sulistyaningsih YC, Hamim H, Kusuma WA. Drug candidates and potential targets of *Curculigo* spp. compounds for treating diabetes mellitus based on network pharmacology, molecular docking and molecular dynamics simulation. J Biomol Struct Dyn. 2023;41:8544–60.
19. Umar AH, Ratnadewi D, Rafi M, Sulistyaningsih YC. Untargeted metabolomics analysis using FTIR and UHPLC-Q-Orbitrap HRMS of two *Curculigo* species and evaluation of their antioxidant and α-glucosidase inhibitory activities. Metabolites. 2021;11:42.
20. Septaningsih DA, Suparto IH, Achmadi SS, Heryanto R, Rafi M. Untargeted metabolomics using UHPLC-Q-Orbitrap HRMS for identifying cytotoxic compounds on MCF-7 breast cancer cells from

Annona muricata Linn leaf extracts as potential anticancer agents. Phytochem Anal. 2024;35:1418–27.

21. Dong Y, Niu Y, Zhang Y, Huo R, Liu Q, Tian X. Exploring the mechanism of action of resveratrol in the treatment of non-small cell lung cancer based on network pharmacology and experimental validation. Sci Technol Food Ind. 2024;45:28–36.
22. Peng H, Huang Z, Li P, Sun Z, Hou X, Li Z, et al. Investigating the efficacy and mechanisms of Jinfu'an decoction in treating non-small cell lung cancer using network pharmacology and *in vitro* and *in vivo* experiments. J Ethnopharmacol. 2024;321:117518.
23. Alsaif G, Tasleem M, Rezgui R, Alshaghdali K, Saeed A, Saeed M. Network pharmacology and molecular docking analysis of *Catharanthus roseus* compounds: Implications for non-small cell lung cancer treatment. J King Saud Univ Sci. 2024;36:103134.
24. Gao Y, Shang B, He Y, Deng W, Wang L, Sui S. The mechanism of Gejie Zhilao Pill in treating tuberculosis based on network pharmacology and molecular docking verification. Front Cell Infect Microbiol. 2024;14.
25. Gong W, Sun P, Li X, Wang X, Zhang X, Cui H, et al. Investigating the molecular mechanisms of resveratrol in treating cardiometabolic multimorbidity: A network pharmacology and bioinformatics approach with molecular docking validation. Nutrients. 2024;16:2488.
26. Zhou Y, Zhang Y, Lian X, Li F, Wang C, Zhu F, et al. Therapeutic target database update 2022: Facilitating drug discovery with enriched comparative data of targeted agents. Nucleic Acids Res. 2022;50:D1398–407.
27. Davis AP, Wiegers TC, Johnson RJ, Sciaky D, Wiegers J, Mattingly CJ. Comparative Toxicogenomics Database (CTD): update 2023. Nucleic Acids Res. 2023;51:D1257–62.
28. Umar AH, Widuri SA, Caecilia Sulistyaningsih Y, Ratnadewi D. Integrating metabolomic analysis, network pharmacology, and molecular docking to underlying pharmacological mechanism and ethnobotanical rationalization for diabetes mellitus: Study on medicinal plant *Fibraurea tinctoria* Lour. Phytochemical Analysis. 2024;0:1–22.
29. Gao K, Chen Z, Zhang N, Jiang P. High throughput virtual screening and validation of plant-based EGFR L858R kinase inhibitors against non-small cell lung cancer: An integrated approach utilizing GC–MS, network pharmacology, docking, and molecular dynamics. Saudi Pharm J. 2024;32:102139.
30. Gurning K, Suratno S, Astuti E, Haryadi W. Untargeted LC/HRMS metabolomics analysis and anticancer activity assay on MCF-7 and A549 cells from *Coleus amboinicus* Lour leaf extract. Iran J Pharm Res. 2024;23:e143494.
31. Sun F, Liu J, Xu J, Tariq A, Wu Y, Li L. Molecular mechanism of Yi-Qi-Yang-Yin-Ye against obesity in rats using network pharmacology, molecular docking, and molecular dynamics simulations. Arab J Chem. 2024;17:105390.
32. Cao M, Zhan M, Jing H, Wang Z, Wang Y, Li X, et al. Network pharmacology and experimental evidence: MAPK signaling pathway is involved in the anti-asthma roles of *Perilla frutescens* leaf. Heliyon. 2024;10:e22971.

33. Zhao Y, Yang G, Ren D, Zhang X, Yin Q, Sun X. Luteolin suppresses growth and migration of human lung cancer cells. Mol Biol Rep. 2011;38:1115–9.
34. Hong Z, Cao X, Li N, Zhang Y, Lan L, Zhou Y, et al. Luteolin is effective in the non-small cell lung cancer model with L858R/T790M EGF receptor mutation and erlotinib resistance. Br J Pharmacol. 2014;171:2842–53.
35. Cho H-J, Ahn K-C, Choi JY, Hwang S-G, Kim W-J, Um H-D, et al. Luteolin acts as a radiosensitizer in non-small cell lung cancer cells by enhancing apoptotic cell death through activation of a p38/ROS/caspase cascade. Int J Oncol. 2015;46:1149–58.
36. Wang X, Chen B, Xu D, Li Z, Liu H, Huang Z, et al. Molecular mechanism and pharmacokinetics of flavonoids in the treatment of resistant EGF receptor-mutated non-small-cell lung cancer: A narrative review. Br J Pharmacol. 2021;178:1388–406.
37. Wang Q, Chen M, Tang X. Luteolin inhibits lung cancer cell migration by negatively regulating TWIST1 and MMP2 through upregulation of miR-106a-5p. Integr Cancer Ther. 2024;23:15347354241247223.
38. Zhang J, Ma Y. Luteolin as a potential therapeutic candidate for lung cancer: Emerging preclinical evidence. Biomed Pharmacother. 2024;176:116909.
39. Moghbeli M. PI3K/AKT pathway as a pivotal regulator of epithelial-mesenchymal transition in lung tumor cells. Cancer Cell Int. 2024;24:165.
40. Wang Z, Xie S, Li L, Liu Z, Zhou W. Schisandrin C inhibits AKT1-regulated cell proliferation in A549 cells. Int Immunopharmacol. 2024;142:113110.
41. Yang Q, Cao C, Wu B, Yang H, Tan T, Shang D, et al. PPIP5K2 facilitates proliferation and metastasis of non-small lung cancer (NSCLC) through AKT signaling pathway. Cancers. 2024;16:590.
42. Mu Y, Liu H, Luo A, Zhang Q. KIFC3 promotes the progression of non–small cell lung cancer cells through the PI3K/Akt pathway. Cancer Cell Int. 2024;24.
43. Chang L, Graham PH, Hao J, Bucci J, Cozzi PJ, Kearsley JH, et al. Emerging roles of radioresistance in prostate cancer metastasis and radiation therapy. Cancer Metastasis Rev. 2014;33:469–96.
44. Xu H, Ma H, Zha L, Li Q, Pan H, Zhang L. Genistein promotes apoptosis of lung cancer cells through the IMPDH2/AKT1 pathway. Am J Transl Res. 2022;14:7040.
45. Hsu P-C, Jablons DM, Yang C-T, You L. Epidermal growth factor receptor (EGFR) pathway, yes-associated protein (YAP) and the regulation of programmed death-ligand 1 (PD-L1) in non-small cell lung cancer (NSCLC). Int J Mol Sci. 2019;20:3821.
46. Humphrey SJ, James DE, Mann M. Protein phosphorylation: A major switch mechanism for metabolic regulation. Trends Endocrinol Metab. 2015;26:676–87.
47. Liu X, Zhang Y, Wang Y, Yang M, Hong F, Yang S. Protein phosphorylation in cancer: Role of nitric oxide signaling pathway. Biomolecules. 2021;11:1009.
48. Singh V, Ram M, Kumar R, Prasad R, Roy BK, Singh KK. Phosphorylation: Implications in cancer. Protein J. 2017;36:1–6.

49. Marcovici I, Vlad D, Buzatu R, Popovici RA, Cosoroaba RM, Chioibas R, et al. Rutin linoleate triggers oxidative stress-mediated cytoplasmic vacuolation in non-small cell lung cancer cells. Life. 2024;14:215.
50. Marghescu A-Ștefania, Leonte DG, Radu AD, Măgheran ED, Tudor AV, Teleagă C, et al. Atypical histopathological aspects of common types of lung cancer—our experience and literature review. Medicina. 2024;60:112.
51. Suster D, Mackinnon AC, Ronen N, Mejbel HA, Harada S, Suster S. Non-small cell lung carcinoma with clear cell features and FGFR3::TACC3 gene rearrangement: Clinicopathologic and next generation sequencing study of 7 cases. Am J Surg Pathol. 2024;48:284.
52. Sreekumar SP, Palanisamy R, Swaminathan R. An approach to segment nuclei and cytoplasm in lung cancer brightfield images using hybrid wwin-unet transformer. J Med Biol Eng. 2024;44:448–59.
53. Wang T, Fan L, Watanabe Y, McNeill PD, Moulton GG, Bangur C, et al. L523S, an RNA-binding protein as a potential therapeutic target for lung cancer. Br J Cancer. 2003;88:887–94.
54. Fan X, Zhang Q, Qin S, Ju S. CircBRIP1: a plasma diagnostic marker for non-small-cell lung cancer. J Cancer Res Clin Oncol. 2024;150:83.
55. Wei Z, Zhao Y, Cai J, Xie Y. The nucleolar protein C1orf131 is a novel gene involved in the progression of lung adenocarcinoma cells through the AKT signalling pathway. Int J Mol Sci. 2024;25:6381.
56. Khan N, Afaq F, Khusro FH, Adhami VM, Suh Y, Mukhtar H. Dual inhibition of PI3K/AKT and mTOR signaling in human non-small cell lung cancer cells by a dietary flavonoid fisetin. Int J Cancer. 2011;130:1695.
57. Phan TKT, Shahbazzadeh F, Pham TTH, Kihara T. Alpha-mangostin inhibits the migration and invasion of A549 lung cancer cells. PeerJ. 2018;6:e5027.
58. Wang JJ, Sanderson BJS, Zhang W. Cytotoxic effect of xanthones from pericarp of the tropical fruit mangosteen (*Garcinia mangostana* Linn.) on human melanoma cells. Food Chem Toxicol. 2011;49:2385–91.
59. Wang A, Zhou F, Li D, Lu J-J, Wang Y, Lin L. γ-Mangostin alleviates liver fibrosis through Sirtuin 3-superoxide-high mobility group box 1 signaling axis. Toxicol Appl Pharmacol. 2019;363:142–53.
60. Tumewu L, Wardana FY, Ilmi H, Permanasari AA, Hafid AF, Widyawaruyanti A. *Cratoxylum sumatranum* stem bark exhibited antimalarial activity by lactate dehydrogenase (LDH) assay. J Basic Clin Physiol Pharmacol. 2021;32:817–22.
61. Suryanto S, Tumewu L, Ilmi H, Hafid AF, Suciati S, Widyawaruyanti A. Antimalarial activity of Cratoxyarborenone E, a prenylated xanthone, isolated from the leaves of *Cratoxylum glaucum* Korth. Pharmacia. 2024;71:1–7.
62. Wardana F, Sari D, Adianti M, Permanasari A, Tumewu L, Nozaki T, et al. *In vitro* anti-amebic activity of cage xanthones from *Cratoxylum sumatranum* stem bark against *Entamoeba histolytica*. Pharmacogn J. 2020;12:452–8.

63. Chen D, Oezguen N, Urvil P, Ferguson C, Dann SM, Savidge TC. Regulation of protein-ligand binding affinity by hydrogen bond pairing. Sci Advan. 2016;2:e1501240.
64. Itoh Y, Nakashima Y, Tsukamoto S, Kurohara T, Suzuki M, Sakae Y, et al. N+-C-H···O Hydrogen bonds in protein-ligand complexes. Sci Rep. 2019;9:767.
65. Yu Y, Wang S, Wang Y, Zhang Q, Zhao L, Wang Y, et al. AKT1 promotes tumorigenesis and metastasis by directly phosphorylating hexokinases. J Cell Biochem. 2024;125:e30613.
66. Chen L, Lu Y, Zhao M, Xu J, Wang Y, Xu Q, et al. A non-canonical role of endothelin converting enzyme 1 (ECE1) in promoting lung cancer development via directly targeting protein kinase B (AKT). J Gene Med. 2024;26:e3612.
67. Zhang W, Hu M-L, Shi X-Y, Chen X-L, Su X, Qi H-Z, et al. Discovery of novel Akt1 inhibitors by an ensemble-based virtual screening method, molecular dynamics simulation, and *in vitro* biological activity testing. Mol Divers. 2024 [cited 2024 Oct 22]; Available from: https://doi.org/10.1007/s11030-023-10788-3
68. Nam A-Y, Joo SH, Khong QT, Park J, Lee NY, Lee S-O, et al. Deoxybouvardin targets EGFR, MET, and AKT signaling to suppress non-small cell lung cancer cells. Sci Rep. 2024;14:20820.
69. Burgess AW. EGFR family: Structure physiology signalling and therapeutic targets. Growth Factors. 2008;26:263–74.
70. Seshacharyulu P, Ponnusamy MP, Haridas D, Jain M, Ganti AK, Batra SK. Targeting the EGFR signaling pathway in cancer therapy. Expert Opin Ther Targets. 2012;16:15–31.
71. Sarrami N, Wuest M, Paiva IM de, Leier S, Lavasanifar A, Wuest F. Immuno-PET imaging of EGFR with 64Cu-NOTA panitumumab in subcutaneous and metastatic nonsmall cell lung cancer xenografts. Mol Pharmaceutics. 2024 [cited 2024 Oct 22]; Available from: https://doi.org/10.1021/acs.molpharmaceut.4c00823
72. Menzel M, Kirchner M, Kluck K, Ball M, Beck S, Allgäuer M, et al. Genomic heterogeneity at baseline is associated with T790M resistance mutations in EGFR-mutated lung cancer treated with the first-/second-generation tyrosine kinase inhibitors. J Pathol Clin Res. 2024;10:e354.
73. Chen Z, Vallega KA, Wang D, Quan Z, Fan S, Wang Q, et al. DNA topoisomerase II inhibition potentiates osimertinib's therapeutic efficacy in EGFR-mutant non–small cell lung cancer models. J Clin Invest. 2024;134.
74. Pal R, Teli G, Sengupta S, Maji L, Purawarga Matada GS. An outlook of docking analysis and structure-activity relationship of pyrimidine-based analogues as EGFR inhibitors against non-small cell lung cancer (NSCLC). J Biomol Struct Dyn. 2024;42:9795–811.
75. Shin G-C, Lee HM, Kim N, Seo S-U, Kim KP, Kim K-H. PRKCSH contributes to TNFSF resistance by extending IGF1R half-life and activation in lung cancer. Exp Mol Med. 2024;56:192–209.
76. Wilt LD, Sobocki BK, Jansen G, Tabeian H, Jong S de, Peters GJ, et al. Mechanisms underlying reversed TRAIL sensitivity in acquired bortezomib-resistant non-small cell lung cancer cells. Cancer Drug Resist. 2024;7:12.

77. Ifandari I, Widyarini S, Nugroho LH, Pratiwi R. Phytochemical analysis and cytotoxic activities of two distinct cultivars of ganyong rhizomes (*Canna indica*) against the WiDr colon cancer cell line. Biodiversitas. 2020;21.
78. Webster R. *In vitro* anticancer activity of native and modified black rice flour against colon cancer cell line. Intern Med. 2022;12:1–4.

Tables

Table 1 and 2 are available in the Supplementary Files section.

Figures

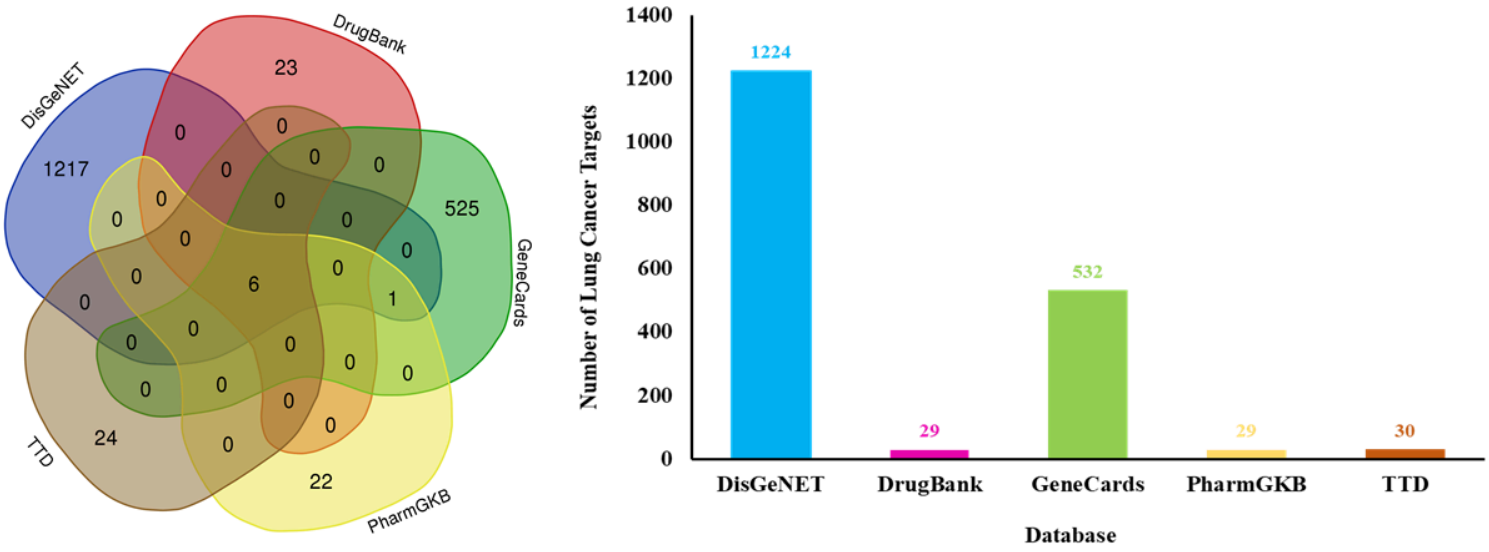

Figure 1

Venn diagram of lung cancer targets using DisGeNet, DrugBank, GeneCards, PharmGKB, and TTD databases.

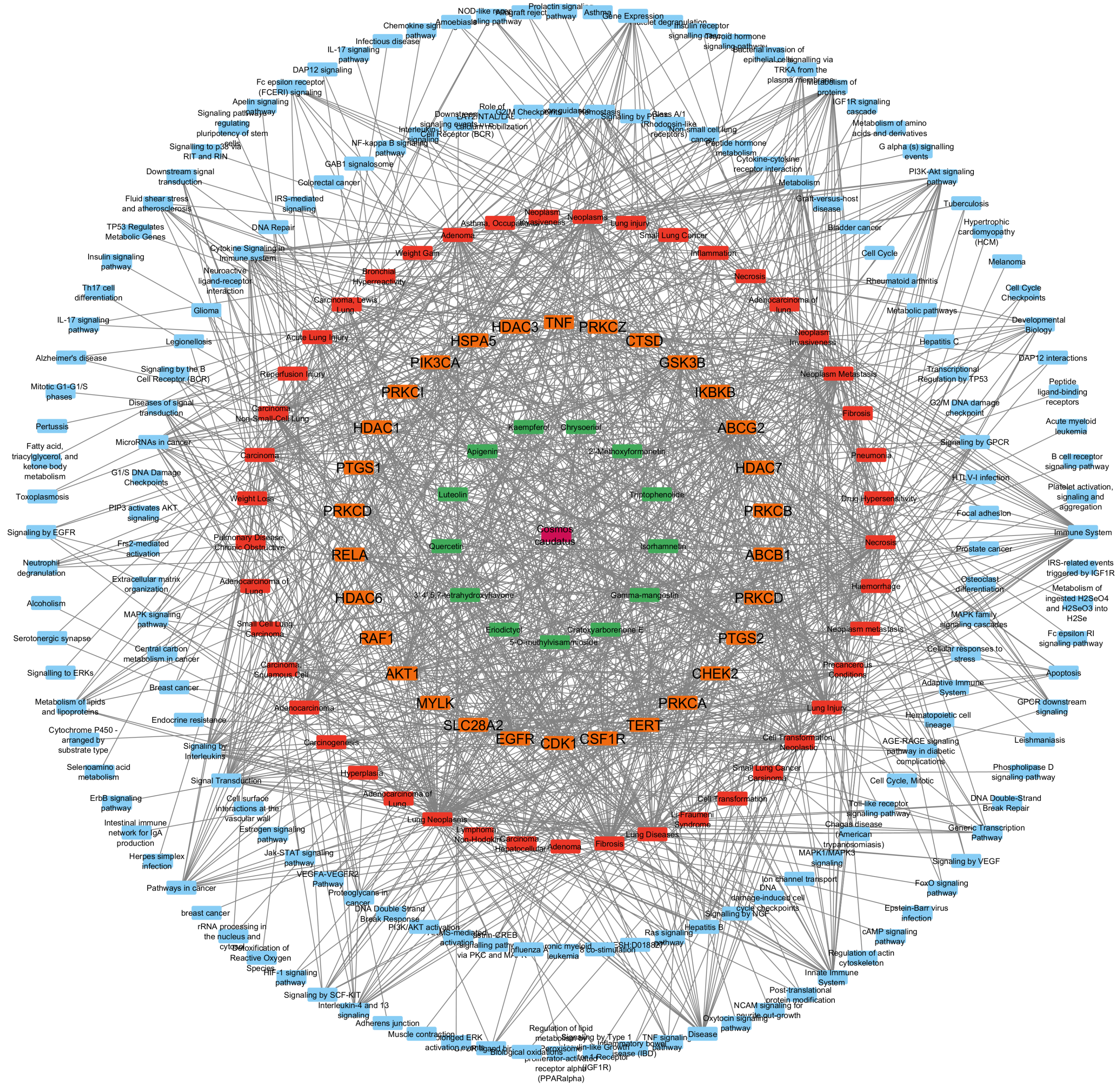

Figure 2

Visualizations of pharmacological networking diagram illustrating the multi-compound-multi-target-multi-disease-multi-pathway interaction of C. caudatus against lung cancer. Pink node (plant), green nodes (compound), orange nodes (target), brown nodes (disease) and blue nodes (pathway).

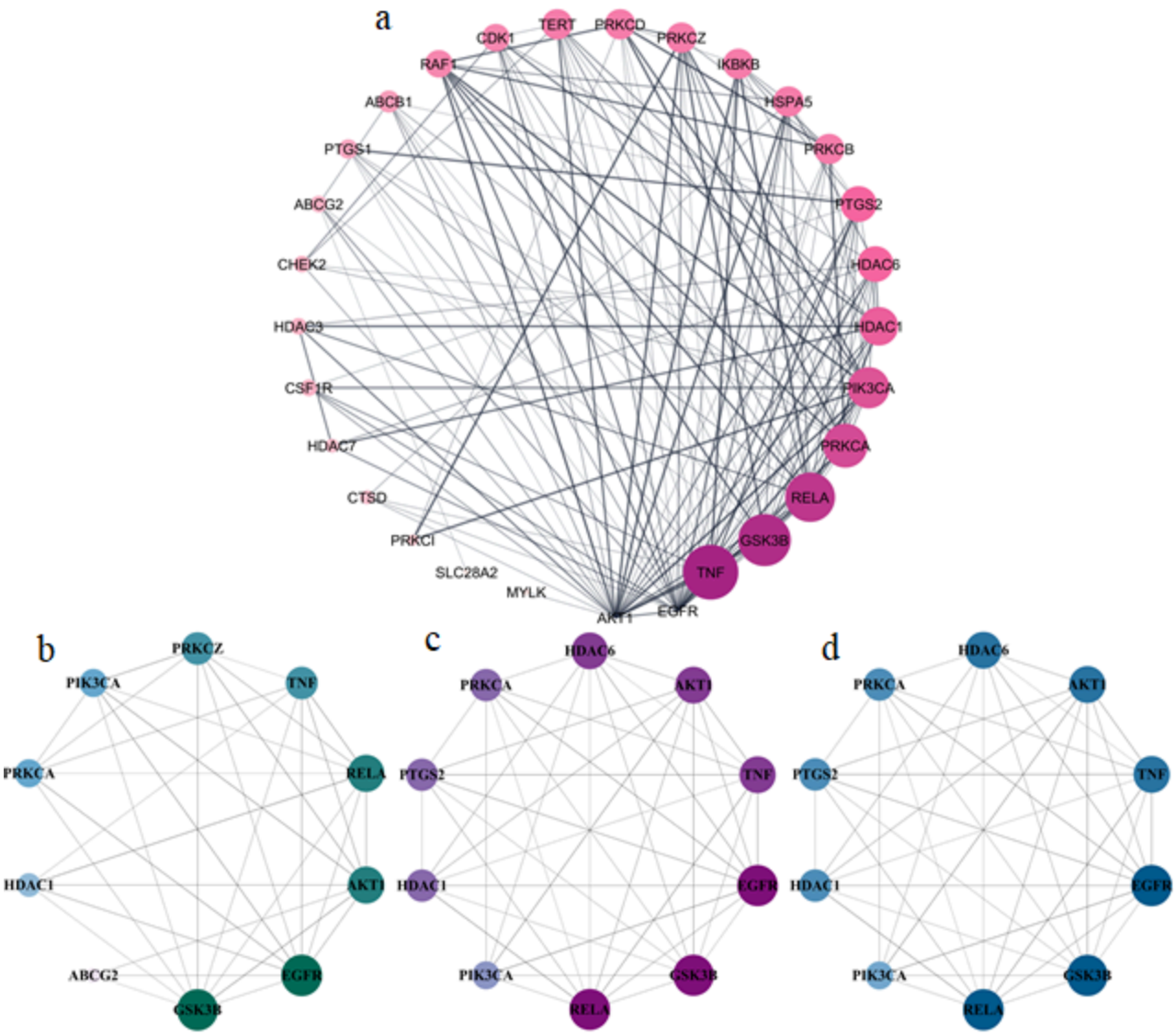

Figure 3

Protein-protein interaction (PPI) network formed in lung cancer. The larger the circle and the lighter the colour, the more degrees the node has (a). Top 10 targets from the topology of degree (b), betweenness centrality (c), and closeness centrality (d).

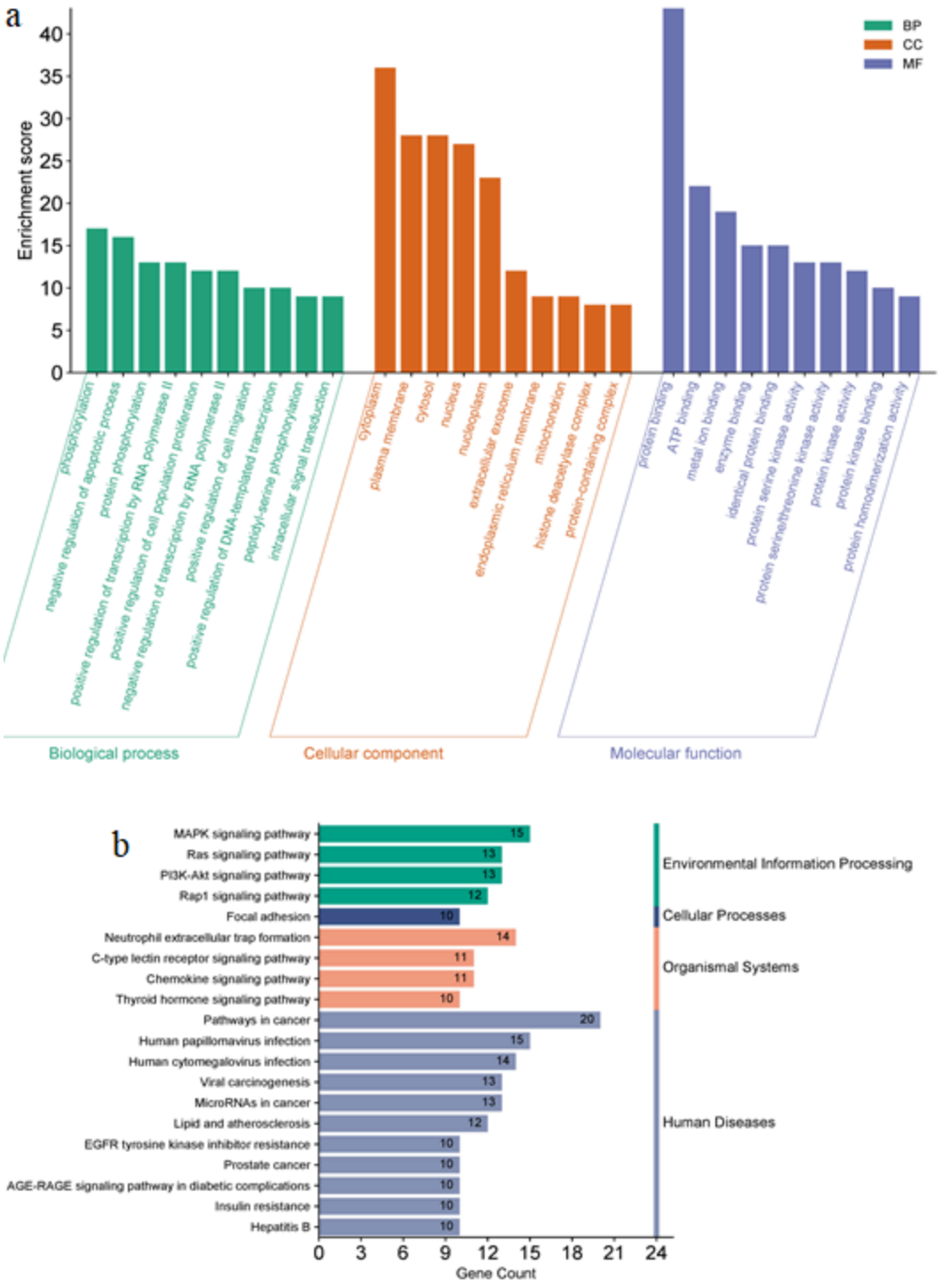

Figure 4

Gene ontology (GO) for cellular components (CC), molecular functions (MF), biological processes (BP), and KEGG pathways, each of which is related to lung cancer.

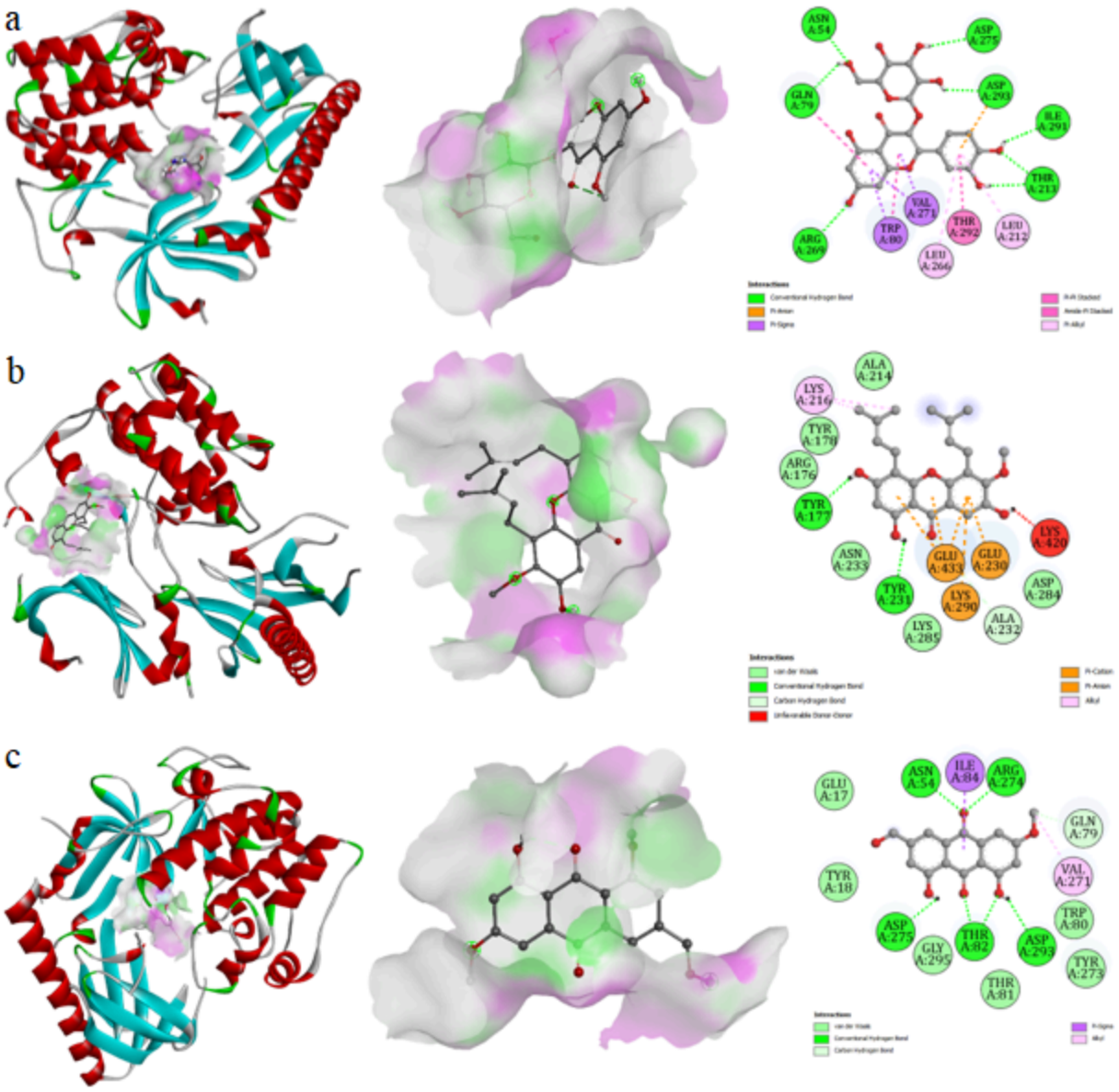

Figure 5

Molecular docking analysis of 2-D and 3-D with the best binding affinity (smallest). Binding between compounds and targets, 3',4',5,7-tetrahydroxyflavone-AKT1 (9C1W) (a), gamma-mangostin-EGFR (3P0V) (b), and cratoxyarborenone E-TNF (1XU1) (c).

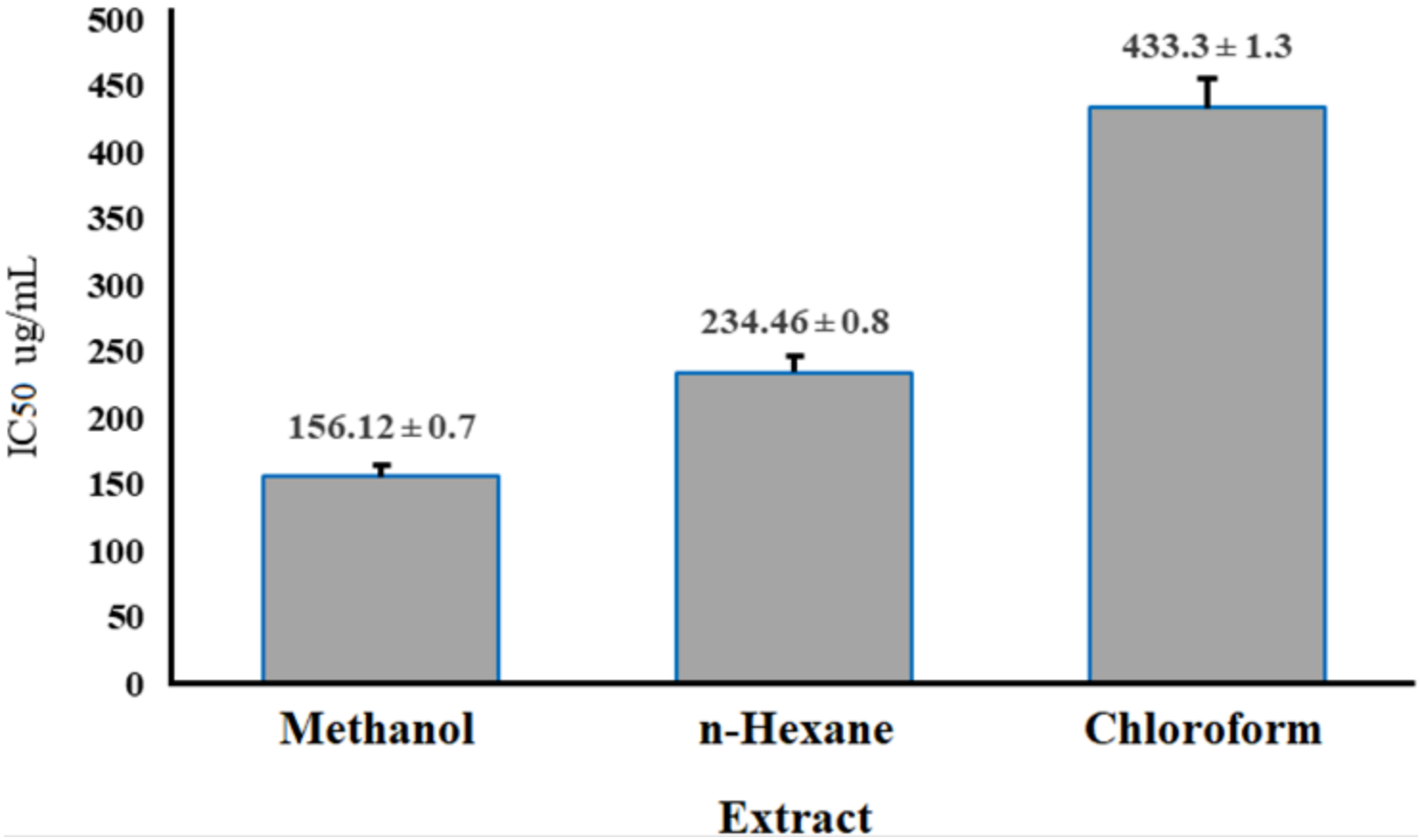

Figure 6

IC_{50} values of extracts in methanol, chloroform, and n-hexane solvents against A549 cells

Supplementary Files

This is a list of supplementary files associated with this preprint. Click to download.

- SupplementaryMaterialJPharmInnovAnonymous.docx
- TableJPharmInnov1.docx
- GA.png